Optics Communications 365 (2016) 215–219

Contents lists available at ScienceDirect

Optics Communications

journal homepage: www.elsevier.com/locate/optcom

Broad-stripe single longitudinal mode laser based on metal slots

Peng Jia, Li Qin, Yongyi Chen*, Jianwei Zhang, Jian Zhang, Xing Zhang, Yugang Zeng, Xiaonan Shan, Yongqiang Ning, Lijun Wang

State Key Laboratory of Luminescence and Application, Changchun Institute of Optics, Fine Mechanics and Physics, Chinese Academy of Sciences, Changchun 130033, China

ARTICLE INFO

Article history:
Received 9 October 2015
Received in revised form
3 December 2015
Accepted 11 December 2015
Available online 18 December 2015

Keywords:
Single-longitudinal-mode
Metal slots
Semiconductor laser

ABSTRACT

Single-longitudinal-mode end-emitting laser with 10 periods of metal slots at around 956 nm has been fabricated. 100 μm wide broad-stripe and ten periods of 9.5 μm periodicity metal slots are defined by i-line lithography and dry etching. Experimentally, continuous-wave power of 213 mW has achieved, at a slope efficiency of 520 mW/A, having a 3 dB spectrum width of less than 0.04 nm at 900 mA, and operating in a stable single longitudinal mode with the side-mode suppression ratio (SMSR) of 42 dB. We prove that metal slots introduce sufficient loss into the cavity to filter out the wanted mode, and is more efficient on our chip structure than traditional slot laser. This paper provides a new method for the realizing high power broad-stripe (~100 μm) laser and array with single longitudinal mode operation.

1. Introduction

Single longitudinal mode semiconductor lasers based on Distributed feedback (DFB) lasers [1–4], distributed Bragg reflection (DBR) lasers [5–7] and external cavity lasers (ECLs) [8,9] have found wide applications in optical interconnection, optical communication, pumping sources of fiber lasers and so on.

In recent years, the Cork and Dublin University put forward a new type of slot-DBR laser diode [10–12], which introduced periodic reflective perturbations structure (slots) into the Fabry–Perot (FP) cavity to supply specific reflectivity property at a certain wavelength, so as to improve the longitudinal-mode characteristics. This type of laser can be easily fabricated and has drawn a lot of attention. Since then, several works [13–16] based on slot-DBR or slot-DFB lasers are reported. Some are multiple longitudinal mode (linewidth~0.7 nm), with high power up to more than 10 W [13–15].

In this paper, we propose a kind of board-stripe high power single longitudinal mode semiconductor laser with metal slots. Different from our previous work of a gain coupled DFB laser based on periodic surface anode canals, basically controlled by electric method demonstrated in Ref. [4], we proved in this paper that, metal slots influence the laser cavity based on a different principle from slot-DBR lasers or slot-DFB lasers: instead of supplying specific wavelength reflectivity demonstrated in Refs. [10–12], metal slots behave as a wavelength filter by introducing loss to unwanted longitude modes. Meanwhile, we have proved our metal slot laser to be more efficient rather than ordinary slot DBR laser. Even though metal in the slots tend to absorb a small part of the lasing energy, the total loss is still less than the high order scattering loss in ordinary slot laser which is usually inevitable and hard to control by i-line lithography. The board-stripe metal slot laser provides a 3 dB spectrum width of less than 0.04 nm and a SMSR up to 42 dB with output power of 213 mW at an injection current of 900 mA, which is the same power level of international reported single longitude mode second order DFB(271 nm periodicity) semiconductor lasers [16]. This type of metal slot laser can be easily fabricated by simple i-line lithography, and doesn't need specific process for preparing V-shape slots [13–15,17], especially the complicated stepper lithography used in Ref. [17]. The wavelength in 956 nm is especially suitable for Yb:SSO crystals demonstrated in Ref. [18] as pumping sources.

2. Experimental methods

The schematic structure of the DBR laser is shown in Fig. 1(a). The chip was fabricated by epitaxial growth using the Metal Organic Chemical Vapor Deposition (MOCVD) method. The fabrication process started with the definition of the photoresist layer for the broad stripes by i-line lithography. The width of the broad-stripes was 100 μm. Then the broad stripes were etched to a depth of 1.4 μm using an inductively coupled plasma etcher. Afterwards, i-line lithography was used to pattern the gratings on the broad-stripes and dry etching was used to form the grating grooves with a depth of 1.2 μm and width of 1.86 μm at a periodicity of 9.5 μm

* Corresponding author.
E-mail address: chenyy@ciomp.ac.cn (Y. Chen).

http://dx.doi.org/10.1016/j.optcom.2015.12.015
0030-4018/

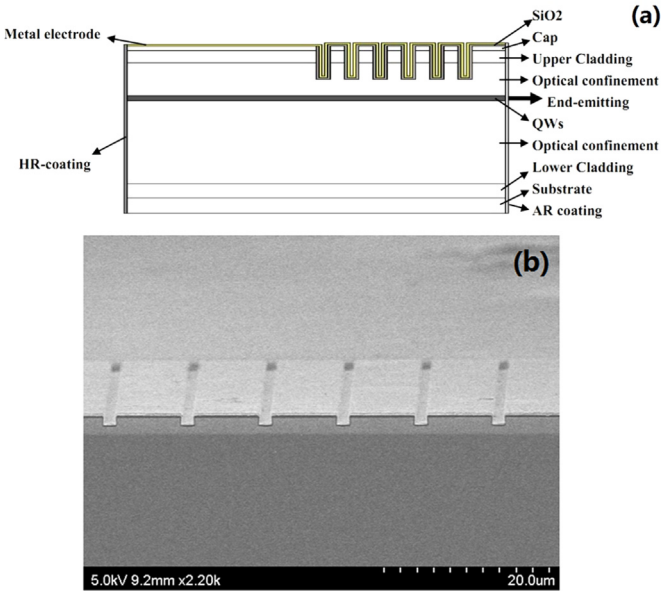

Fig. 1. (a) Schematic structure of metal slots laser; (b) Scanning electron microscope picture of metal slots, covered by a 200 nm isolation layer and a 300 nm metal electrode layer.

for ten periods at one side of the laser cavity. The lengths of the laser cavity and metal slots region are 1.8 mm and 0.2 mm respectively. Notice that our metal slots were still about 105 μm away from the emitting facet, far enough for cleavage processing. After that, 200 nm SiO_2 was deposited using PECVD. The side walls of the grating grooves of SiO_2 were 100 nm thick after this process. Then the broad-stripes were metal contacted for 300 nm gold. Gold is also introduced to the grating grooves, yet isolated by the layer of insulated SiO_2. Fig. 1(b) shows the metal slots under SEM. Finally, the chips were cleavage and high reflectivity (about 99.2% reflectivity) films were deposited on none emitting facet of the cavity without the gratings, then anti-reflectivity (about 5% reflectivity) films were deposited on the emitting facet of the cavity near the grating region. For comparison purposes, FP lasers were also prepared on the same wafer.

3. Results and discussion

3.1. Results

To test the laser diodes in continuous-wave (CW) operation, the lasers are mounted p-side down on Cu c-mount heat sinks and placed on a water-cooling unit to hold at a stationary temperature of 20 °C. As a comparison, a common FP laser without metal slots and not filmed on the cavity facet is also tested. The spectra is measured by YOKOGAWA AQ6370C optical spectrum analyzer coupled by a 10 μm core diameter fiber at 0.02 nm resolution, which means $\pm$0.02 nm testament error.

The CW power–current characteristics and spectrum of devices are shown in Fig. 2(a) and (b). The threshold current and slope efficiency of device with metal slots are 600 mA and 520 mW/A. There is a kinking at about 1000 mA which represents a clear transition from basic longitude mode lasing to multiple mode lasing [17]. The output spectra shows a stable single mode performance at an injection current from 700 mA to 900 mA, as shown in Fig. 2(b). The 3 dB spectrum width is 0.04 nm, already beyond our testament error. The SMSR is about 42 dB. Output power of metal slots laser with an injection current of 900 mA is 213 mW.

The threshold current and slope efficiency of the normal FP laser are about 500 mA and 546 mW/A, as shown in Fig. 2(c). The F–P laser is typical multiple longitudinal mode operation. Fig. 2 (d) shows the output spectra of F–P laser with center wavelength at 953.84 nm and the 3 dB spectrum width of 3.18 nm at injection current of 900 mA. Comparing our metal slots laser with F–P laser, the spectral width is reduced by about 80 times. The metal slots are beneficial to compress the line-width of FP lasers.

3.2. Discussion

Scattering matrix method [19] is used for analysis the S parameters of the metal slots and total threshold modal gain. Consider a single grating unit (shown in Fig. 3), the input power of the basic waveguide mode at port i is A_i, the reflective power of the basic waveguide mode is B_i, $i=1,2$. A matrix can be developed to express the outputs as a weighted combination of the inputs:

$$B_i = \sum S_{ij}A_j,\ i, j = 1, 2$$

where the S_{ij} are scattering coefficients.

So that we have the scattering matrix equation:

$$B_i = \sum S_{ij}A_j,\ i,\ j = 1, 2\ \begin{bmatrix} B_1 \\ B_2 \end{bmatrix} = \begin{bmatrix} S_{11} & S_{12} \\ S_{21} & S_{22} \end{bmatrix}\begin{bmatrix} A_1 \\ A_2 \end{bmatrix} \quad (1)$$

In this two-port grating unit, we have S_{11} and S_{22} as the reflection coefficient r_1 and r_2. The power reflection coefficients in this case are $|S_{11}|^2$ and $|S_{22}|^2$, respectively. In Fig.3, as a symmetric structure, $S_{11}=S_{22}$, $S_{12}=S_{21}$. But in a metal slot, the two-port grating unit cannot be estimated as a low loss system. The scattering matrix must be changed to transmission matrix for further analysis. The transformation relationship between scattering matrix and transmission matrix according to [19] is:

$$T_{11} = \frac{1}{S_{21}}$$
$$T_{12} = -\frac{S_{22}}{S_{21}}$$
$$T_{21} = \frac{S_{11}}{S_{21}}$$
$$T_{22} = -\frac{S_{11}S_{22} - S_{12}S_{21}}{S_{21}} \quad (2)$$

For ten duration periods, the total transmission matrix can be expressed as:

$$T_{grating} = \begin{bmatrix} T_{g,11} & T_{g,12} \\ T_{g,21} & T_{g,22} \end{bmatrix} = \begin{bmatrix} T_{11} & T_{12} \\ T_{21} & T_{22} \end{bmatrix}^{10} \quad (3)$$

Then, the total scattering matrix $S_{grating}$ can be expressed from $T_{grating}$:

$$S_{grating} = \begin{bmatrix} S_{g,11} & S_{g,12} \\ S_{g,21} & S_{g,22} \end{bmatrix} = \frac{1}{T_{g,11}}\begin{bmatrix} T_{g,21} & T_{g,11}T_{g,22} - T_{g,12}T_{g,21} \\ 1 & -T_{g,12} \end{bmatrix} \quad (4)$$

So the total power of basic waveguide mode reflected by the 10 periods of metal slots is $|S_{g,11}|^2$ and the total power of basic waveguide mode transmitted through the 10 periods of metal slots is $|S_{g,21}|^2$. Finally the total loss, including metal loss, high order waveguide mode diffractive loss and scattering loss can be calculated by total input power minus the transmitted power and the reflected power: $1-|S_{g,11}|^2-|S_{g,21}|^2$. The scattering matrix elements S_{11} and S_{21} were numerically calculated by finite element method supplied by commercial software COMSOL multiphysics. Then the data were post processed by programming.

Fig. 4 shows the calculated total loss and reflection properties

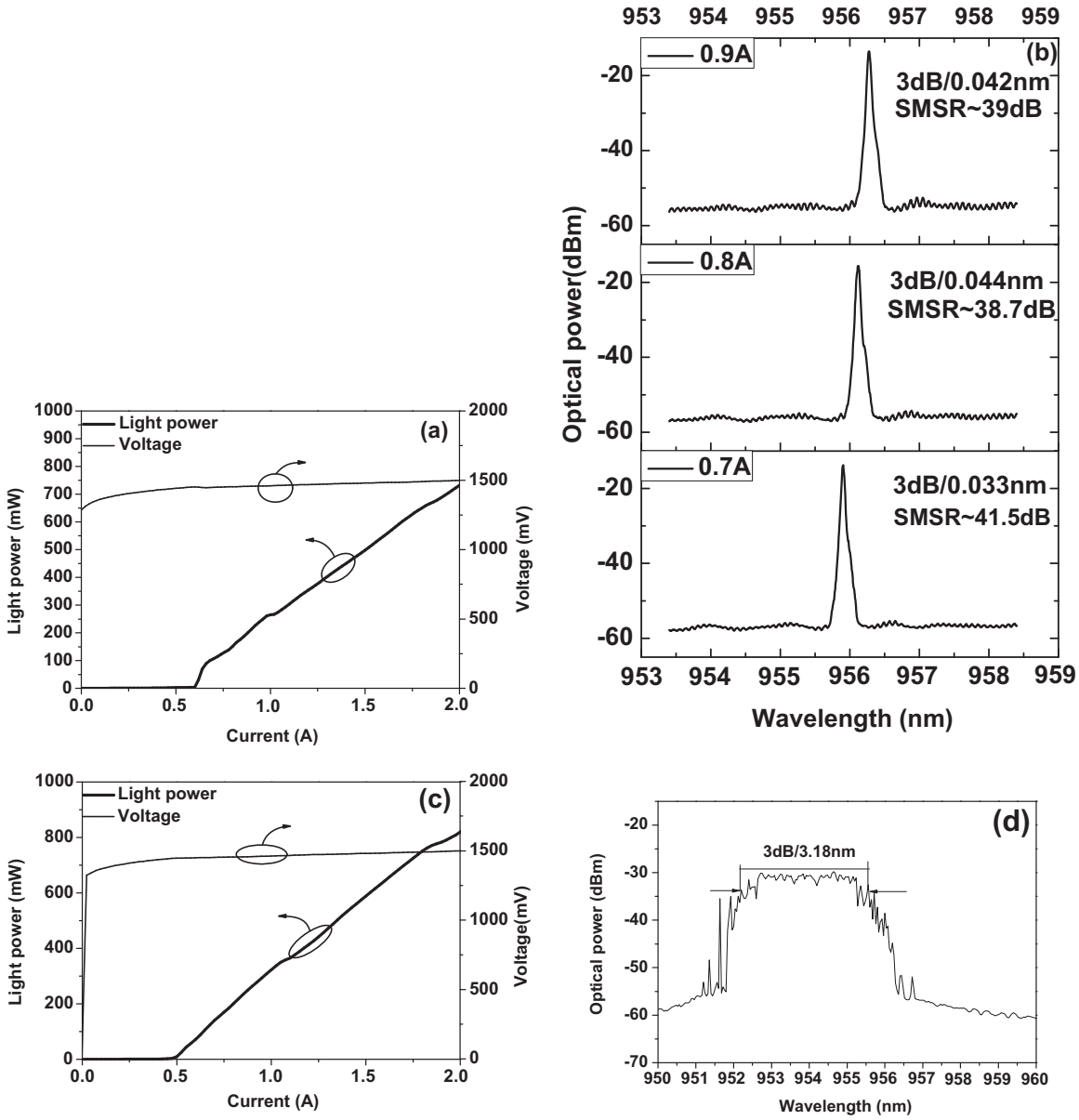

Fig. 2. (a) CW power–voltage–current characteristics of metal slots lasers; (b) Optical spectra of metal slots lasers at 20 °C; (c) CW power–voltage–current characteristics of FP lasers; (d) Optical spectra of FP lasers at 900 mA for 20 °C.

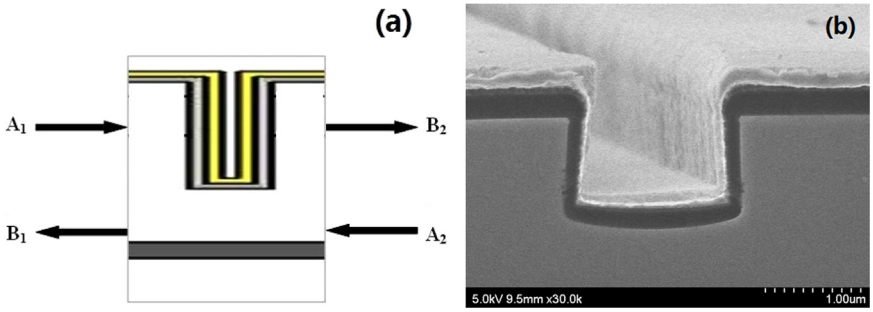

Fig. 3. (a) Schematic structure of a period grating structure with input basic waveguide mode and reflective basic waveguide mode; (b) Scanning electron microscope picture of a period grating structure, covered by a 200 nm isolation layer and a 300 nm metal layer.

by the metal slots when etching depth changes, the etching width is fixed at 1.86 μm.

We find that, in Fig. 4(a), as etching depth increases, the loss of ten periodicity metal slots increases. That is because when etching deeper to the waveguide, more power couple into the metal slots, increasing the scattering loss. The loss meets a minimum at the wavelength 955.8 nm of 47% and 952.1 nm of 30.4%, but since the gain peak is around 955 nm, the wavelength of 952.1 nm needs a larger current density to reach threshold gain before lasing. So the wavelength 955.8 nm is the theoretical lasing wavelength, which

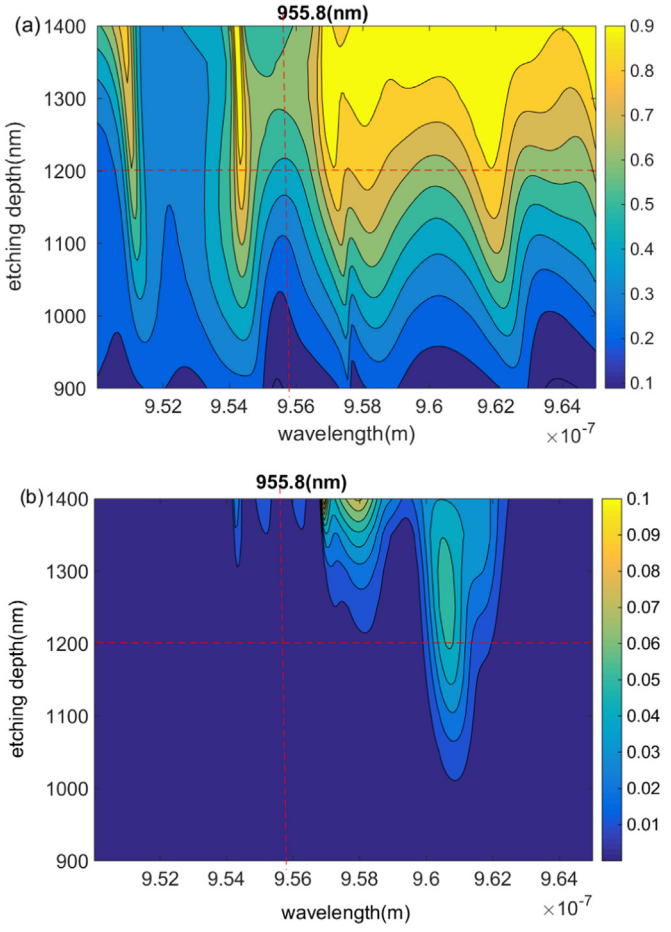

Fig. 4. The total loss (a) and reflection properties (b) of the metal slots when the etching width is fixed at 1.86 μm.

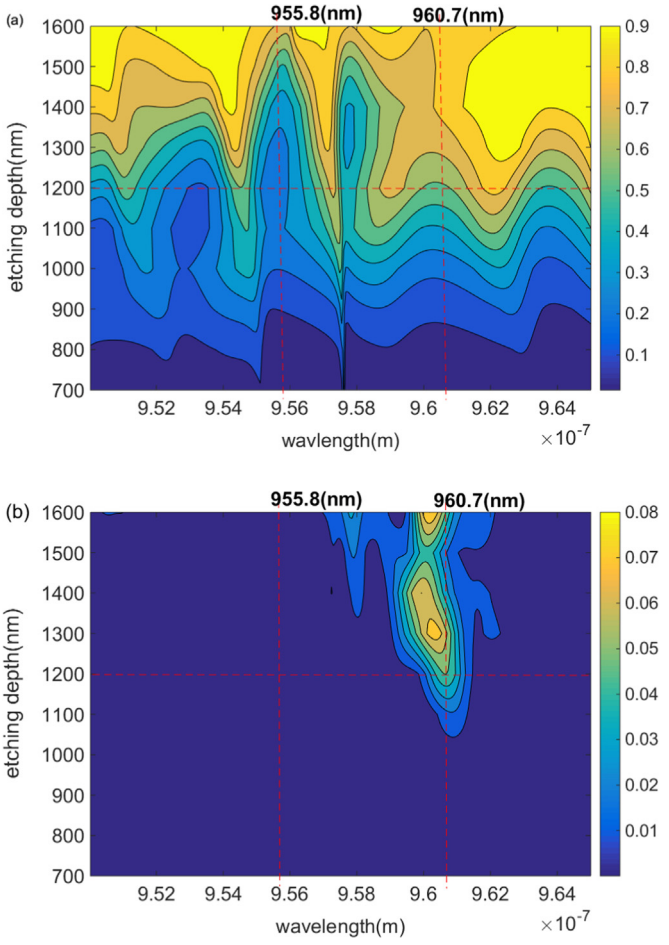

Fig. 5. The total loss (a) and reflection properties (b) of the slots without metal when the etching width is fixed at 1.86 μm for comparison purpose.

is quite close to our experimental test results of 955.9 nm to 956.3 nm as shown in Fig. 2(b), proving our simulating to be accurate. The little difference is probably caused by three reasons: the theoretical refractive index might be different with our chip grown by MOCVD; current injection and heat accumulation may also lead to fluctuations of the chip's refractive index, which is also reflected by Fig. 2(b) that, under different current injection, the laser wavelength shifts from 955.9 nm to 956.3 nm.

Moreover, we can see a reflection peak zone at about 960.7 nm in Fig. 4(b). This peak zone is the specific wavelength reflection zone when the metal slots works as distribute Bragg reflectors mentioned in Ref. [20]. At this wavelength metal slots acts as an effective reflection mirror. But since the total loss is much larger (67.5%), lasing at this wavelength is not stable. On the other hand, metal slots does not play a reflection role at around 956 nm since they do not obey odd numbers of quarter wavelength, so it is obvious that the reflectivity supplied by these 10 periodicities of metal slots is very little, especially for less than 0.12% at numerical lasing wavelength 955.8 nm when the etching depth is 1.2 μm and almost not changed as etching depth increases. That means our metal slots laser works not because of feedback of slot DBRs, but because of the minimum total loss. As etching depth increases, the largest mode reflectivity increase rapidly to about 10%. This is because the deeper the grating grooves are, the larger the mode reflectivity differences are, and meanwhile, grating walls are deep into the waveguide, when metal in the gratings begins to supply mirror reflection to the basic waveguide mode.

To compare with our metal slot laser with ordinary slot lasers, we also show the calculated total loss (Fig. 5(a)) and reflection properties (Fig. 5(b)) for slots properties at a same etching width of 1.86 μm with a same ten slots in Fig. 4. It is apparent from Fig. 5 (b) that, the ordinary slot has a reflection peak of 5% around 960.7 nm when etching depth of 1.2 μm and etching width of 1.86 μm were fixed, which should be the lasing wavelength if proper anti-reflection coating was deposited. However, this kind of traditional slot laser suffers from total loss about 59% of the lasing mode energy. This means that, even though metal slots bring absorption to the total output power, our metal slot laser is still more efficient (47% total loss) than ordinary slot laser (59% total loss) at respective lasing wavelength. High order scattering loss, which takes the main part of total loss usually determined by etching width and etching width, is usually inevitable and hard to control by i-line lithography. That makes traditional slot laser not so efficient on our chip structure. Meanwhile, we can see from Fig. 5 (b) that, the slot laser reflection peak drifts a little around 960.7 nm when etching depth is changed. That is because of two reasons: on one hand, effective index in the waveguide changes when etching depth changes, and a changing effective index in the slots tend to drift the reflection peak according to odd number of quarter wavelength reflection condition. On the other hand, high order scattering light tend to bring a phase shift which might destruct the odd number of quarter wavelength reflection condition.

According to basic rectangular waveguide mode theory [21], the relationship between propagation constant β, and transverse wavenumbers k_x, k_y of the optical mode and vacuum wavenumber k_0 should satisfy:

$$\beta^2 = k_0{}^2 - (k_x{}^2 + k_y{}^2) \quad (5)$$

The propagation constant β is decided by the laser cavity and metal slots which should have the least total loss. For a given β, the frequency is locked. Meanwhile the transverse mode of k_y and vacuum wavenumber k_0 are also locked according to the solution of Maxwell equations by a given single frequency. Then according to formula (5), the lateral mode is also locked to a fixed k_x. That ensures the mode stability before gain saturation and explains our single mode metal slots laser to have a large range of working current from 0.7 A to 0.9 A.

4. Conclusions

A broad-stripe metal slots laser, providing a single longitudinal mode emission with 3 dB spectrum width of less than 0.04 nm and side mode suppression ratio (SMSR) of 42 dB at output power about 213 mW has been presented. This type of metal slot laser can be easily fabricated by simple i-line lithography, and does not need specific process for preparing V-shape slots, thus reduces the cost. We have proved that our metal slots laser has an intrinsic difference from slot laser: the wavelength narrowing and longitude mode selecting are based on introducing loss to unwanted modes, not based on optical feedbacks of the basic waveguide mode, and is more efficient at designed wavelength with total loss smaller than traditional slot laser on our chip. The fabrication technology of the metal slots laser is simple and low cost. It provides a new method for mass production for single longitudinal mode semiconductor laser. Future works include optimizing the structure of the metal slots and to test the devices with a more precise line-width equipment.

Acknowledgments

This work was supported by the National Natural Science Foundation of China (61234004, 61434005, 61176045, 61306086, 61474118, 61474010, 11404327 and 61306059) and the sustentation fund of Jilin Provincial Science and Technology Development Plan (20140101172JC, 20130206006GX, 20140520132JH and 20140101206JC-02).

Reference

[1] J.X. Shi, L. Qin, Y. Liu, N. Zhang, J. Zhang, L.S. Zhang, P. Jia, Y.Q. Ning, Y.G. Zeng, J. L. Zhang, L.J. Wang, Chin. Sci. Bull. 57 (2012) 2083.
[2] K. Dridi, A. Benhsaien, J. Zhang, K. Hinzer, T.J. Hall, Opt. Express 22 (2014) 19087.
[3] J.S. Kim, J.H. Lee, S.U. Hong, H.S. Kwack, B.S. Choi, D.K. Oh, IEEE Photonics Technol. Lett. 18 (2006) 595.
[4] Y.Y. Chen, P. Jia, J. Zhang, L. Qin, H. Chen, Fg Gao, X. Zhang, X.N. Shan, Y.Q. Ning, L.J. Wang, Appl. Opt. 54 (2015) 8863.
[5] R.K. Price, J.J. Borchardt, V.C. Elarde, R.B. Swint, J.J. Coleman, IEEE Photonics Technol. Lett. 18 (2006) 97.
[6] J.W. Zimmerman, R.K. Price, U. Reddy, N.L. Dias, J.J. Coleman, IEEE J. Sel. Top. Quantum Electron. 19 (2013) 1503712.
[7] B. Sumpf, J. Fricke, M. Maiwald, A. Müller, P. Ressel, F. Bugge, G. Erbert, G. Tränkle, Semicond. Sci. Technol. 29 (2014) 045025.
[8] A.I. Bawamia, G. Blume, B. Eppich, A. Ginolas, S. Spiesserger, M. Thomas, B. Sumpf, G. Erbert, IEEE Photonics Technol. Lett. 23 (2011) 1676.
[9] S. Jetté-Charbonneau, P. Berini, Appl. Phys. Lett. 91 (2007) 181114.
[10] Q.Y. Lu, W.H. Guo, M. Nawrocka, A. Abdullaev, C. Daunt, J. O'Callaghan, M. Lynch, V. Weldon, F. Peters, J.F. Donegan, Opt. Express 19 (2011) B140.
[11] W.H. Guo, Q.Y. Lu, M. Nawrocka, A. Abdullaev, J. O'Callaghan, M. Lynch, V. Weldon, J.F. Donegan, IEEE Photonics Technol. Lett. 24 (2012) 634.
[12] B. Corbett, C. Percival, P. Lambkin, IEEE J. Quantum Electron. 41 (2005) 490.
[13] J. Decker, P. Crump, J. Fricke, A. Maassdorf, G. Erbert, G. Trankle, IEEE Photonics Technol. Lett. 26 (2014) 829.
[14] J. Fricke, W. John, A. Klehr, P. Ressel, L. Weixelbaum, H. Wenzei, G. Erbert, Semicond. Sci. Technol. 27 (2012) 055009.
[15] P. Crump, C.M. Schultz, H. Wenzel, G. Erbert, G. Trankle, J. Phys. D – Appl. Phys. 46 (2013) 013001.
[16] A. Klehr, H. Wenzel, O. Brox, F. Bugge, G. Erbert, T.-P. Nguyen, G. Trankle, Opt. Express 15 (2007) 11364.
[17] J. Fricke, H. Wenzel, M. Matalla, A. Klehr, G. Erbert, Semicond. Sci. Technol. 20 (2005) 1149.
[18] C.C. Liu, Y.G. Wang, J. Liu, L.H. Zheng, L.B. Su, J. Xu, Opt. Commun. 285 (6) (2012) 1352–1355.
[19] W.S. Chang, Fundamentals of Guided-Wave Optoelectronic Devices, Cambridge University Press, London, 2009.
[20] Q.Y. Lu, W.H. Guo, D. Byrne, J.F. Donegan, IEEE Photonics Technol. Lett. 22 (2010) 787.
[21] T. Suhara, Semiconductor Laser Fundamentals, Springer, Berlin, 2004.